Original article

Nuclear Medicine Communications

Feasibility of simultaneous ^{18}F-FDG PET/MRI for the quantitative volumetric and metabolic measurements of abdominal fat tissues using fat segmentation

Hyung-Jun Im[a,d], Jin Chul Paeng[a], Gi Jeong Cheon[a,c], Euishin E. Kim[d,e], Jae Sung Lee[a], Jin Mo Goo[b,c], Keon Wook Kang[a,c], June-Key Chung[a,c] and Dong Soo Lee[a,d]

Background **Quantification of volume and inflammatory activity in the fat tissue is important because these are closely related to type 2 diabetes mellitus and cardiovascular disease. Fluorine-18 fluorodeoxyglucose (^{18}F-FDG) PET/computed tomography (CT) has been utilized to measure the metabolic activity of fat tissue. In this study, we assessed the feasibility of simultaneous PET/magnetic resonance (MR) in metabolic and volumetric measurements of fat tissue and the potential advantage over PET/CT.**

Methods **Twenty-four healthy individuals were enrolled, who underwent simultaneous ^{18}F-FDG PET/MRI. Twenty-five ^{18}F-FDG PET/CT scans were selected. Isocontour volumes of interest (VOIs) were used to segment and separate visceral fat (VF) and abdominal subcutaneous fat (SF) in using the MR image (T1 DIXON VIBE sequence) of PET/MR and the CT image of PET/CT. Volume, mean standardized uptake value of VF, and SF VOIs were calculated.**

Results **Overlap between ^{18}F-FDG PET and VF VOI was better in ^{18}F-FDG PET/MR than PET/CT. The mean standardized uptake value of VF was associated with the degree of intestinal uptake on ^{18}F-FDG PET/CT, but not on ^{18}F-FDG PET/MR. Volumetric and metabolic measurements using ^{18}F-FDG PET/MR showed an excellent reproducibility, with a high intraclass correlation coefficient between different observers (0.951–0.997). The measured metabolic activity was higher in VF than SF.**

Conclusion **We established a method for the quantitative measurement of volume and metabolic status of abdominal VF and SF using simultaneous ^{18}F-FDG PET/MR. ^{18}F-FDG PET/MR has an advantage over ^{18}F-FDG PET/CT in terms of being less confounded by intestinal uptake. This method could be used to assess the inflammatory activity of fat tissue, which is a major risk factor for type 2 diabetes mellitus and cardiovascular disease. *Nucl Med Commun* 37:616–622 Copyright © 2016 Wolters Kluwer Health, Inc. All rights reserved.**

Nuclear Medicine Communications 2016, **37**:616–622

Keywords: fluorine-18 fluorodeoxyglucose, inflammation, insulin resistance, PET/MR, visceral fat tissue

Departments of [a]Nuclear Medicine, [b]Radiology, Seoul National University College of Medicine, [c]Cancer Research Institute, Seoul National University College of Medicine, [d]Department of Molecular Medicine and Biopharmaceutical Sciences, Graduate School of Convergence Science and Technology, and College of Medicine or College of Pharmacy, Seoul National University, Seoul, Korea and [e]Department of Radiological Sciences, University of California, Irvine, California, USA

Correspondence to Gi Jeong Cheon, MD, PhD, Department of Nuclear Medicine, Seoul National University College of Medicine, 101 Daehak-ro, Jongno-gu, Seoul 110-744, Korea
Tel: + 82 2 2072 3386; fax: + 82 2 745 7690; e-mail: larrycheon@gmail.com

Received 22 May 2015 **Revised** 2 January 2016 **Accepted** 7 January 2016

Introduction

Obesity is related to the risks of insulin resistance, type 2 diabetes mellitus (T2DM), and cardiovascular disease [1]. The close association between visceral fat (VF) and insulin resistance is well documented in both obese nondiabetic subjects and T2DM patients [2–4]. Also, inflammation in subcutaneous fat (SF) is related to insulin resistance [5]. Production of various inflammatory cytokines and recruitment and activation of inflammatory cells in fat tissue are considered a linkage between obesity and insulin resistance [6,7].

Fluorine-18 fluorodeoxyglucose (^{18}F-FDG) can be accumulated in inflammatory/infectious focus mainly because of recruited and activated macrophages [8]. Accordingly, ^{18}F-FDG PET/computed tomography (CT) has been used in the detection and monitoring of the efficacy of treatment in various types of inflammatory/infectious diseases such as osteomyelitis [9], prosthesis infection [10], fever of unknown origin [11], and sarcoidosis [12]. In one report, ^{18}F-FDG PET/CT showed higher ^{18}F-FDG uptake in VF than SF in clinical observation, which could be attributed to the obese mouse model experiment that showed different degrees of inflammatory cell activation [13]. Thus, measured degree of inflammation in adipose tissue using ^{18}F-FDG PET could be utilized as a biomarker predicting T2DM or cardiovascular diseases in obesity. However, quantification of ^{18}F-FDG uptake in VF on ^{18}F-FDG PET/CT could be hampered by difficulty in discriminating intestinal uptake, partly caused by sequential (not simultaneous) acquisition of PET/CT.

 DOI: 10.1097/MNM.0000000000000488

Recently, the magnetic field compatible PET component was developed by substituting a photomultiplier tube for an avalanche photodiode. This has enabled the development and commercialization of simultaneous PET/magnetic resonance image (MR). Commercial simultaneous PET/MR is now under clinical validation [14]. The simultaneous PET/MR system has several intrinsic advantages over the PET/CT system, which are lower radiation dose, higher soft tissue resolution of anatomical image, and possibility of using a novel multifunctional PET/MR probe, in addition to simultaneous acquisition of anatomical image and PET. The property of simultaneous acquisition of PET and MR is not the most important feature of simultaneous PET/MR, but the property is essential to measure the metabolism of VF. In PET/CT, there is a time difference of a few minutes between PET and CT because of the sequential acquisition of PET and CT, which could cause poor registration of the intestine. In PET/MR, the intestine can be registered more accurately because of the simultaneous acquisition of PET and MR. In this study, we investigated the feasibility of measuring volume and ^{18}F-FDG uptake of abdominal fat tissues using simultaneous PET/MR.

Methods

Participants

After first installation of simultaneous PET/MR in our institute in October 2012, 44 volunteer participants underwent ^{18}F-FDG PET/MRI for 2 months. Among these, 24 participants who had neither current oncologic disease nor abnormal metabolically active lesions in the abdominal cavity were enrolled for analysis of our study retrospectively. During the same period, 3178 participants underwent ^{18}F-FDG PET/CT scans in the same institute. Among these, 33 participants were selected randomly, but eight were excluded because of the presence of current oncologic diseases (two lung cancers, two stomach cancers, one colon cancer, and three lymphomas). The study design and exemption of informed consent were approved by the Institutional Review Board of Seoul National University Hospital.

^{18}F-FDG PET/MR and ^{18}F-FDG PET/CT imaging protocol

After fasting for at least 6 h, blood glucose level was checked. Appropriate blood glucose criterion was less than 180 mg/dl. Antidiabetic medication was discontinued 1 day before the examination. Approximately 5.18 MBq/kg (0.14 mCi/kg) of ^{18}F-FDG was administered intravenously. Imaging acquisition was performed ~60 min after an ^{18}F-FDG injection using a Biograph mCT scanner (Siemens Medical Solution, Knoxville, Tennessee, USA) for ^{18}F-FDG PET/CT or a Biograph mMR scanner (Siemens Medical Solution) for ^{18}F-FDG PET/MR. In ^{18}F-FDG PET/CT imaging, CT scans were performed for attenuation correction and anatomical correlation (120 kVp, 40 mAs, pitches of 1.2). Then, ^{18}F-FDG PET acquisitions were performed with 1 min per bed position from the proximal thigh to the skull base. ^{18}F-FDG PET reconstructions were performed using a point spread function-based iterative algorithm (TrueX, two iterations, 21 subsets; TrueX, Siemens Medical Solution, Erlangen, Germany) and a time-of-flight function with a matrix size of 200×200 and a voxel size of $4.07 \times 4.07 \times 4.07$ mm. For ^{18}F-FDG PET/MR, PET acquisition and MR acquisitions were performed simultaneously with 3 min per bed position from the skull base to the proximal thigh. The scan time per bed position of PET/MR was optimized to obtain a comparable image quality with PET/CT. ^{18}F-FDG PET reconstructions were performed using three-dimensional (3D) ordered subset expectation maximization (two iterations, 21 subsets) with a matrix of 172×172 and a voxel size of $4.17 \times 4.17 \times 2.03$ mm. During ^{18}F-FDG PET acquisition, MRI was acquired with a two-point Dixon 3D volumetric interpolated breath-hold examination T1-weighted MR sequence (DIXON VIBE, Siemens Medical Solution, Erlangen, Germany). A μ-map was produced from the DIXON VIBE image and used for attenuation correction of the ^{18}F-FDG PET image.

Fat segmentation

All image analyses were carried out using PMOD software version 3.4 (PMOD Technologies, Zürich, Switzerland). In both PET/MR and PET/CT, the visceral and subcutaneous area was separated using an automatic 3D isocontour volume of interest (VOI), which can separate abdominal soft tissue wall and SF [using a threshold of 0.086 cm^{-1} for PET/MR, Hounsfield Unit (HU) of −30 for PET/CT [15], Fig. 1a], and then the abdominal area was selected using cube VOI from the lower margin of the left diaphragm to the upper margin of the bladder. In each inside and outside of the VOI, automatic 3D isocontour VOI was applied to segment VF (Fig. 1b) and SF (Fig. 1c). Used thresholds for fat segmentation were 0.086 cm^{-1} in PET/MR, and Hounsfield Unit (HU) between −190 and −30 in PET/CT [15]. Volume and mean standardized uptake value (SUV) of VF and SF VOIs were calculated. All measurements were performed twice by different operators on different days for PET/MR. SUV was calculated as follows: SUV = [decay corrected activity (kBq) per ml of tissue volume]/[injected ^{18}F-FDG activity (kBq) per body weights (g)].

As the intestines are major organs that may cause confounding ^{18}F-FDG uptake in VF, the degree of overlap between intestinal contour and ^{18}F-FDG uptake was graded as follows in both PET/CT and PET/MR: one or more nonoverlapped segment between PET and CT (or MR) as grade 1 (poor overlap), three or more nonoverlapped foci as grade 2 (fair overlap), and less than three nonoverlapped foci as grade 3 (excellent overlap) (Fig. 2). Also, the degree of intestinal uptake in ^{18}F-FDG PET was graded in both PET/CT and PET/MR as follows: grade 1 as lower than the liver uptake, grade 2 as segmental intestinal uptake with an intensity similar to or higher than the liver uptake, grade 3 as diffuse intestinal

Fig. 1

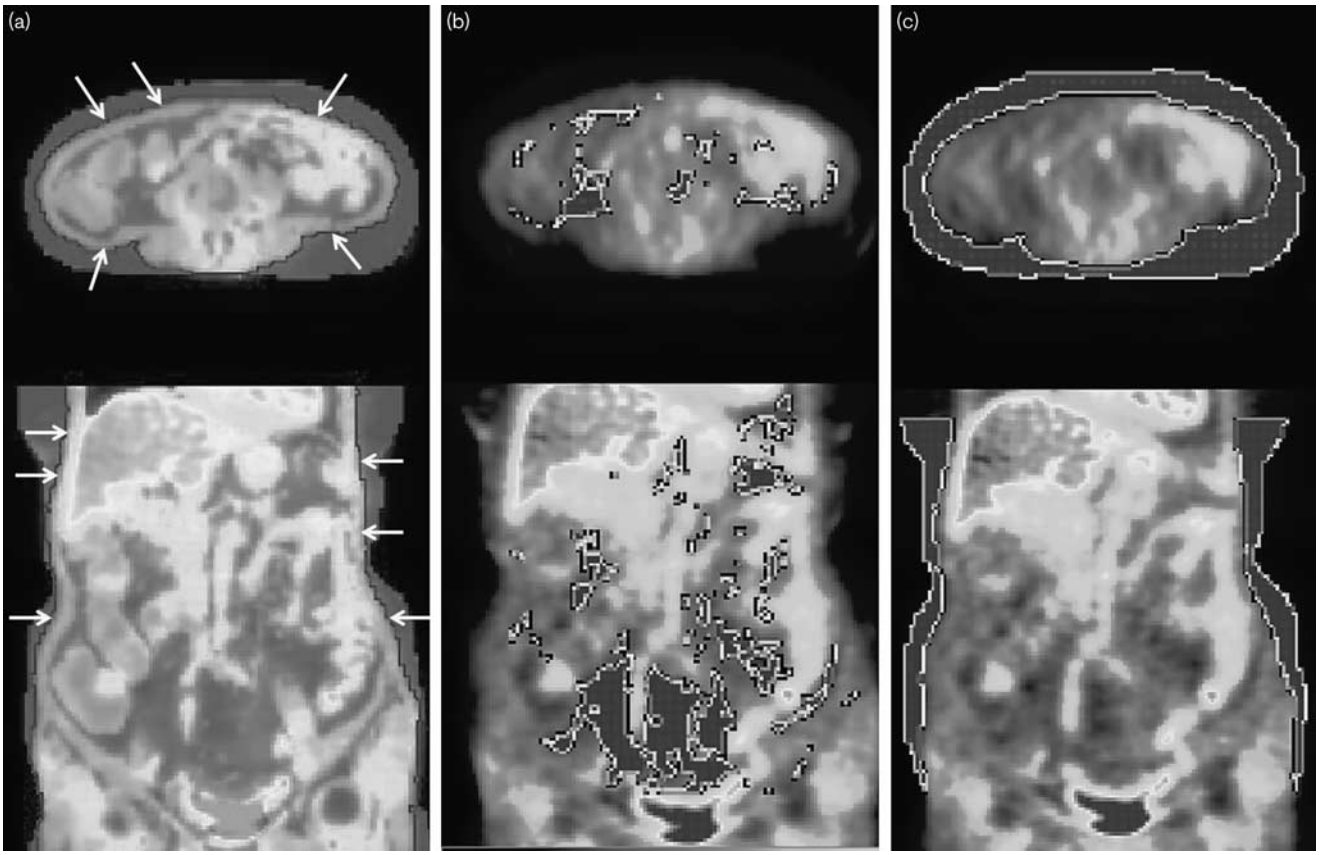

Method for fat segmentation and measurement. 3D isocontour VOI (white arrows) separating soft tissue and subcutaneous fat tissue is shown on the axial and coronal fusion image of the μ-map and ^{18}F-FDG PET image (a). Using the 3D isocontour method, VF VOI (b) and SF VOI (c) were prepared and fused with the ^{18}F-FDG PET image. CT, computed tomography; ^{18}F-FDG, fluorine-18 fluorodeoxyglucose; SF, subcutaneous fat; VF, visceral fat; VOI, volume of interest.

uptake with an intensity similar to the liver uptake, and grade 4 as diffuse intestinal uptake with higher intensity than the liver uptake.

Statistical analysis

Statistical analysis was carried out using SPSS (version 18.0; IBM Software, Chicago, Illinois, USA) and a value of P less than 0.05 was considered statistically significant. Intraclass correlation analysis and the limits of agreement according to Bland and Altman were carried out between the first and second measurements of the mean SUV and volume of fat VOIs. Repeatability coefficient was also calculated, which is the value below which the absolute differences between two measurements would lie with 0.95 probability. The χ^2-test was carried out to determine the overlap grades of ^{18}F-FDG PET/CT and PET/MR, and the numbers of participants in each grade of intestinal uptake. The Kruskal–Wallis test was used to evaluate the association between grade of intestinal uptake and the mean SUV of VF. An unpaired t-test was carried out to compare the means between two groups.

Results

Participants

Basic characteristics including age, sex, fasting glucose level, and BMI were not significantly different between participants who underwent ^{18}F-FDG PET/CT and ^{18}F-FDG PET/MR (Table 1).

Overlap between intestinal contour and ^{18}F-FDG uptake

To evaluate the independence of ^{18}F-FDG uptake of VF and the intestine, the overlap between contour and ^{18}F-FDG uptake of the intestine was graded in ^{18}F-FDG PET/CT and PET/MR. In ^{18}F-FDG PET/CT, nine participants showed poor overlap (grade 3), 14 participants showed fair overlap (grade 2), and only two participants showed excellent overlap (grade 1). In ^{18}F-FDG PET/MR, no participant showed poor overlap, nine participants showed fair overlap, and 15 participants showed excellent overlap. On the basis of the χ^2-test, the overlap between intestinal contour and ^{18}F-FDG uptake was better in ^{18}F-FDG PET/MR than PET/CT ($P < 0.0001$).

Fig. 2

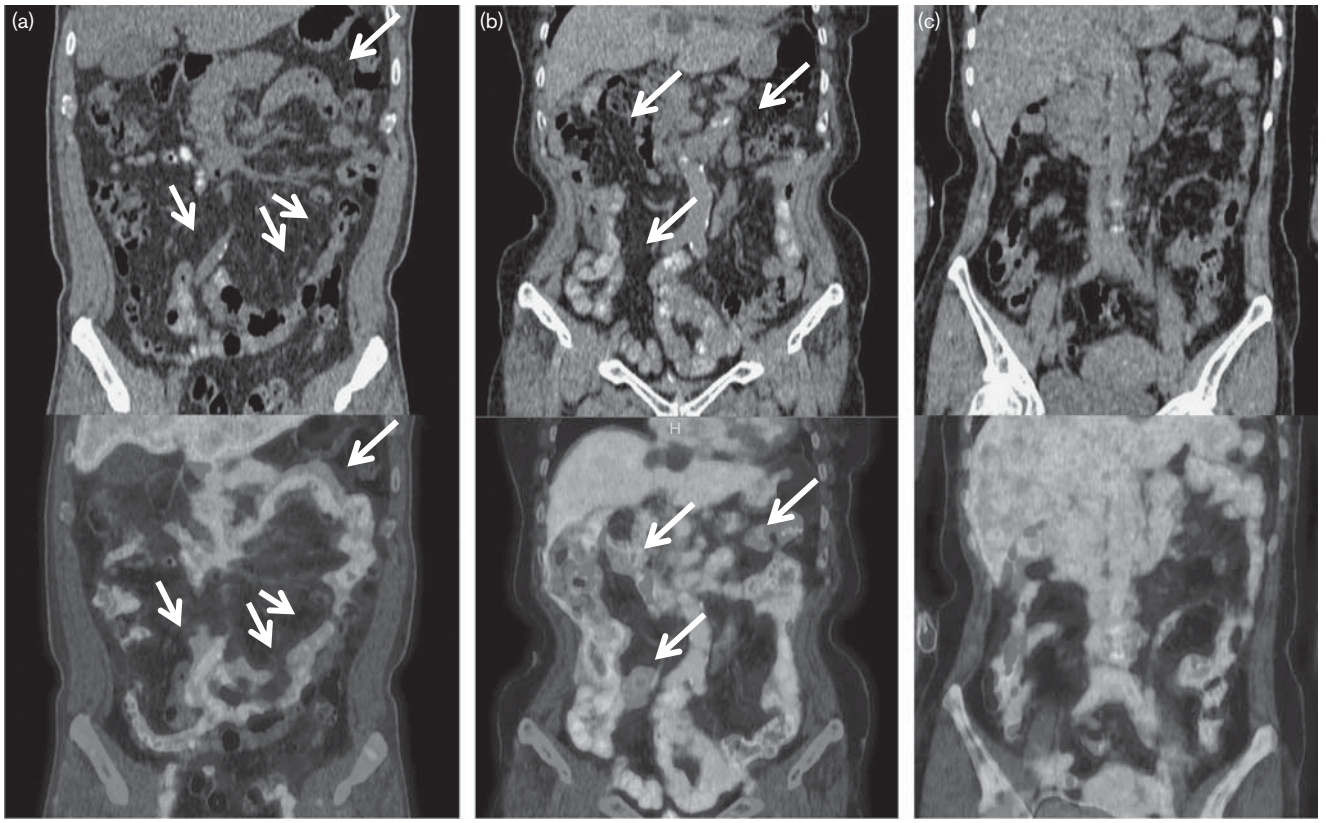

Degree of overlap between intestinal contour and ^{18}F-FDG uptake. The images are representative coronal CT (upper row) and fused ^{18}F-FDG PET/CT image (lower row) of poor overlap (grade 1, a), fair overlap (grade 2, b), and excellent overlap (grade 3, c). White arrows indicate mismatches between intestinal contour and ^{18}F-FDG uptake. CT, computed tomography; ^{18}F-FDG, fluorine-18 fluorodeoxyglucose.

Table 1 Characteristics of the participants

	^{18}F-FDG PET/CT	^{18}F-FDG PET/MR	Difference
Number of participants	25	24	P=NS
Age (mean±SD)	54.2±14.7	61.8±13.1	P=NS
Sex			
Male	15	14	P=NS
Female	10	10	
Fasting glucose(mg/ml)	114.7±37.0	115.2±31.2	P=NS
BMI (kg/m^2)	23.9±2.9	23.7±2.9	P=NS

CT, computed tomography; ^{18}F-FDG, fluorine-18 fluorodeoxyglucose; NS, nonsignificant.

Relationship between intestinal ^{18}F-FDG uptake and VF VOI

For further evaluation of the impact of the intestinal ^{18}F-FDG uptake in the measurement of ^{18}F-FDG uptake of VF VOI, the correlation of the grade of intestinal ^{18}F-FDG uptake and the mean SUV of VF VOI was analyzed. The number of participants in each grade of intestinal uptake was 6 (grade 1), 10 (grade 2), 7 (grade 3), and 2 (grade 4) in ^{18}F-FDG PET/CT and 10, 8, 4, and 2 in PET/MR, respectively. There was no significant difference between ^{18}F-FDG PET/CT and PET/MR in terms of the distribution of participants in each grade (P=NS). There was a significant association between the mean SUV and grade of intestinal uptake in ^{18}F-FDG PET/CT (P=0.03), but this was not significant in ^{18}F-FDG PET/MR (P=0.85, Fig. 3).

Measurement of volume and metabolic status of fat tissues in ^{18}F-FDG PET/MR and PET/CT

In ^{18}F-FDG PET/MR, the volume and mean SUV of VF and SF VOI in ^{18}F-FDG PET/MR were measured. Volumes of VF and SF were 1115.69±389.55 and 2823.88±1283.52 ml (mean±SD), respectively. The mean SUV of VF and SF were 0.50±0.06 and 0.29±0.06, respectively. The mean SUV of VF was significantly higher than that of SF (P<0.0001).

In ^{18}F-FDG PET/CT, the volumes of VF and SF were 1052.58±446.96 and 2039.54±976.36 ml (mean±SD), respectively. The mean SUV of VF and SF were 0.89±0.17 and 0.53±0.13, respectively. Also, in PET/CT, the mean SUV of VF was significantly higher than that of SF also in PET/CT (P<0.0001). The difference in the mean SUV between PET/CT and PET/MR was probably caused by the use of a different reconstruction

Fig. 3

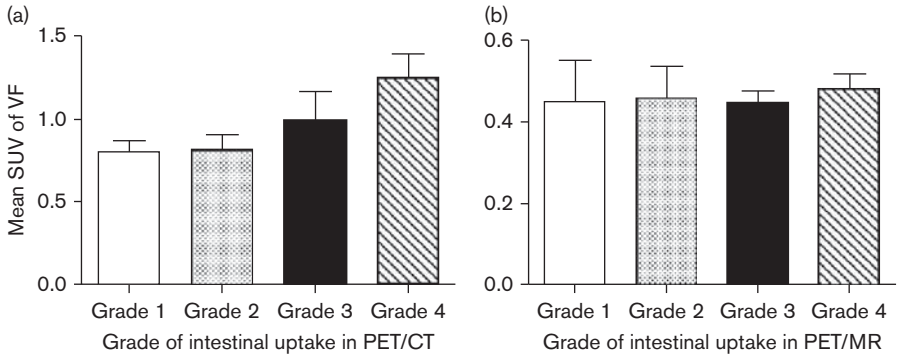

Correlation of grade of intestinal uptake and the mean SUV of VF VOI. The degree of intestinal uptake in ^{18}F-FDG PET is correlated with the mean SUV of VF VOI in ^{18}F-FDG PET/CT (a), but not in PET/MR (b). Participants with a higher grade of intestinal uptake have a higher mean SUV of VF VOI in ^{18}F-FDG PET/CT, but the grade of intestinal uptake does not affect the mean SUV of VF VOI in ^{18}F-FDG PET/MR. (grade 1 = lower than the liver uptake, grade 2 = segmental intestinal uptake with an intensity similar to or higher than the liver, grade 3 = diffuse intestinal uptake with similar intensity with the liver, and grade 4 = diffuse intestinal uptake with higher intensity than the liver). CT, computed tomography; ^{18}F-FDG, fluorine-18 fluorodeoxyglucose; MR, magnetic resonance; SUV, standardized uptake value; VF, visceral fat; VOI, volume of interest.

method because point spread function was applied only in PET/CT [16].

Reproducibility of measurement of volume and metabolic status of fat tissues in ^{18}F-FDG PET/MR

The mean SUV and volume of VF and SF were measured twice and intraclass correlation coefficients were calculated. All measurements showed an excellent reproducibility with a high intraclass correlation coefficient (0.951–0.997) (Fig. 4, Table 2). In the Bland–Altman plot, two measurements showed excellent agreement with 95% limits of agreement ranging from −0.032 to 0.046 in the mean SUV and −157.53 to 99.58 ml in the volume of VF (Fig. 4). Repeatability coefficients were 0.039 for the mean SUV and 128.56 ml for volume.

Discussion

In this study, we have introduced a reliable, reproducible method to measure volume and ^{18}F-FDG uptake in fat tissues using simultaneous ^{18}F-FDG PET/MR for the first time. As abdominal obesity is known to be related to risks of metabolic and cardiovascular disorders, many methods were introduced to assess the amount of fat tissue, such as anthropometric measurement, dual-energy X-ray absorptiometry [17], CT [15], and MR [18]. CT and MR have the advantages of separating and quantifying subcutaneous and VF volume over other methods. Measurement of VF at the umbilicus level using CT is the most commonly used method to correlate the amount of VF with metabolic disorder and cardiovascular risk [15]. Volume of adipose tissue can also be measured using CT and is considered a gold standard to measure VF [19,20]. However, CT has a disadvantage: a risk of ionizing radiation. Without the shortcoming, MRI can also measure fat volume. Two-point DIXON sequence imaging is the most widely used method to separate and measure volume of fat and water. As the sequence was used in the simultaneous PET/MR system to create an attenuation map (μ-map), which has been found to be feasible [21], the authors used a μ-map to segment fat tissue. In addition to measuring the volume of abdominal fat tissue using a μ-map of the MR image, at the same time, we measured the metabolic parameter of abdominal fat tissue using simultaneous ^{18}F-FDG PET/MR and evaluated the significance of the parameter.

^{18}F-FDG PET was used to assess the metabolic rate of glucose of fat tissue under conditions of euglycemic hyperinsulinemia [22,23]. In these studies, the anatomical reference was the corresponding MR image, which was obtained separately with ^{18}F-FDG PET, and 12 to 18 manually drawn region of interest in fat tissue was used for analysis. However, this measurement may not be objective because of manual registration of two separately acquired images and use of manually drawn region of interest. In addition, these studies did not assess the basal level of glucose uptake and thus cannot be applied to the general population. In one report, ^{18}F-FDG uptake in fat tissue was measured using an automated fat segmentation method in ^{18}F-FDG PET/CT [13]. In this study, a binary fat mask was generated using CT images and ^{18}F-FDG uptake in the fat mask was measured, and thus this method could be more objective than the previous researches. However, we found from our study that a substantial amount of intestinal ^{18}F-FDG uptake is overlaid in VF VOI of ^{18}F-FDG PET/CT. Moreover, measured ^{18}F-FDG uptake in VF VOI of ^{18}F-FDG PET/CT is associated with intestinal ^{18}F-FDG uptake itself. However, in most of our cases, intestinal ^{18}F-FDG uptake was not overlapped on the VF VOI in ^{18}F-FDG PET/MR, and there was no association between intestinal

Fig. 4

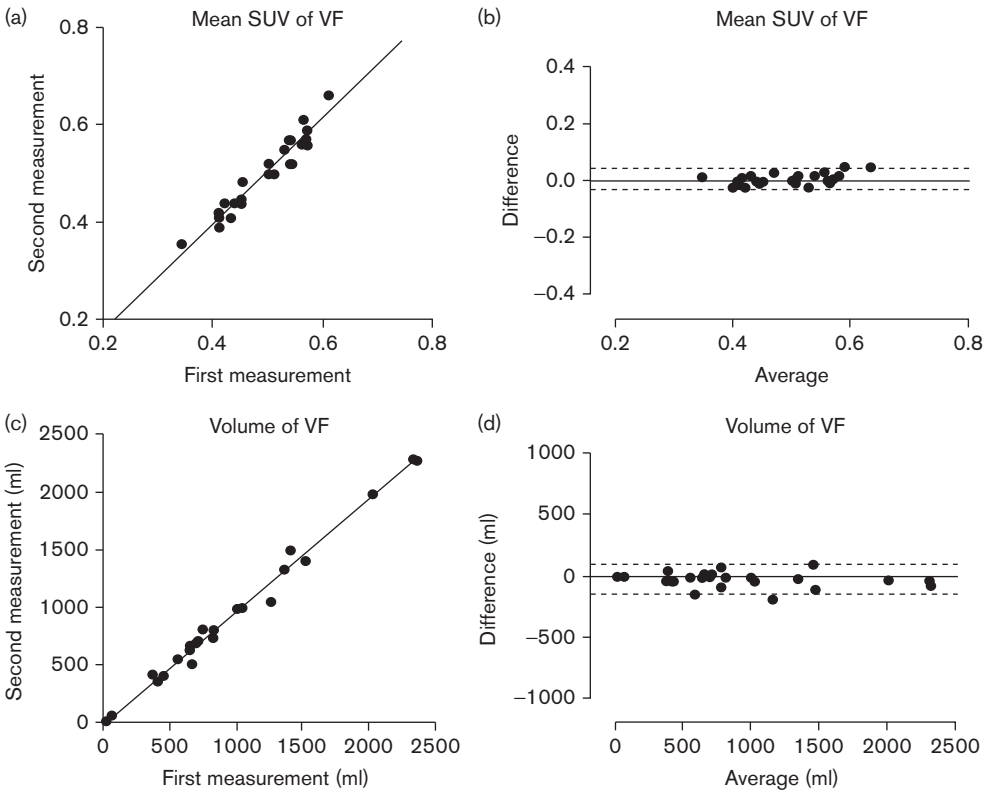

Reproducibility of measurement of VF VOI in ^{18}F-FDG PET/MR. Scatter plots with a linear regression line and Bland–Altman plot between the first and the second measurement of mean SUV (a, b) and volume (c, d) of VF VOI are shown. Measurement of volume and the mean SUV of VF VOI in ^{18}F-FDG PET/MR showed excellent reproducibility. Dotted lines represent the 95% limit of agreement. CT, computed tomography; ^{18}F-FDG, fluorine-18 fluorodeoxyglucose; MR, magnetic resonance; SUV, standardized uptake value; VF, visceral fat; VOI, volume of interest.

Table 2 Intraclass correlation of VF and SF measurements in ^{18}F-FDG PET/MR

	Type	ICC	95% CI	*P* value
Volume	VF	0.997	0.992–0.999	< 0.0001
	SF	0.951	0.888–0.979	< 0.0001
Mean SUV	VF	0.959	0.906–0.983	< 0.0001
	SF	0.987	0.969–0.994	< 0.0001

CI, confidence interval; ^{18}F-FDG, fluorine-18 fluorodeoxyglucose; ICC, intraclass correlation coefficient; MR, magnetic resonance; SF, subcutaneous fat; SUV, standardized uptake value; VF, visceral fat.

^{18}F-FDG uptake and ^{18}F-FDG uptake of VF VOI. Also, the mean SUV of VF was not associated with the volume of VF in ^{18}F-FDG PET/MR (P=0.324), indicating that measured ^{18}F-FDG uptake in VF is not related to a spill-over effect. Thus, simultaneous ^{18}F-FDG PET/MR has superior properties compared with ^{18}F-FDG PET/CT in measuring the volume and ^{18}F-FDG uptake of fat tissues.

In the present study, the mean SUV of VF was higher than that of SF, which is in agreement with a previous report [13]. Christen *et al.* [13] showed that the stromal vascular cell fraction (rich in inflammatory cells) of VF had higher gene expression related to glucose metabolism than SF. Thus, we could speculate that measured metabolic activity from ^{18}F-FDG PET/MR could also reflect the inflammatory process in the VF and SF [13,20].

Inflammation in fat tissue has been shown to be a link between obesity and T2DM and cardiovascular diseases. Thus, low-dose aspirin or statin could be considered to reduce the risk of the complications. However, as not all obese patients have T2DM or cardiovascular disease, administration of preventive anti-inflammatory drugs cannot be justified. Thus, if a higher risk of T2DM or cardiovascular disease in obese patients can be predicted, more aggressive behavioral modification and preventive administration of anti-inflammatory drug can be considered in those with a higher risk. Although assessment of the serum level of C-reactive protein is the most widely accepted method to monitor the systemic inflammatory condition, its elevation cannot be localized and can be easily confounded by temporary inflammatory or infectious condition such as common cold [24]. Therefore, ^{18}F-FDG PET/MR could be used as a specific inflammatory marker of fat tissues and furthermore as a predictor of T2DM or cardiovascular disease after validation with a prospective study with larger numbers

of patients. In addition, using the segmentation method in the present study, other tracers that can target inflammation such as macrophage or translocator protein targeting agents can be used to evaluate inflammation of fat tissue.

There are several limitations in this study. A medical history of hypertension, or hyperlipidemia and other laboratory examinations such as creatinine clearance that could affect ^{18}F-FDG uptake in VF was not evaluated because of the retrospective design of the present study. The initial hypothesis that ^{18}F-FDG uptake in fat tissue reflects the degree of inflammation could not be proved because biopsy of fat tissue or C-reactive protein measurement was not performed in this preliminary study. Finally, ^{18}F-FDG PET/MR and PET/CT were not done in the same participant, and thus the capability of fat segmentation and feasibility could not be compared directly. Also, there was a difference between PET/CT and PET/MR in scan time per bed, which could be a confounding factor.

Conclusion

Simultaneous ^{18}F-FDG PET/MR has an advantage over PET/CT in the quantitative measurement of volume and metabolic status of VF and SF in terms of being less influenced by intestinal ^{18}F-FDG uptake. The metabolic activity of VF was higher than SF ^{18}F-FDG PET/MR. The method for the quantitative measurement of fat tissue volume and metabolism, which we have suggested here, could be used to assess the characteristics of obesity.

Acknowledgements

This research was supported by a grant from the Korea Health Technology R&D Project through the Korea Health Industry Development Institute (KHIDI), funded by the Ministry of Health & Welfare, Republic of Korea (grant number: HI14C1072).

Conflicts of interest

There are no conflicts of interest.

References

1 Smith SR, Lovejoy JC, Greenway F, Ryan D, deJonge L, de la Bretonne J, *et al*. Contributions of total body fat, abdominal subcutaneous adipose tissue compartments, and visceral adipose tissue to the metabolic complications of obesity. *Metabolism* 2001; **50**:425–435.
2 Miyazaki Y, DeFronzo RA. Visceral fat dominant distribution in male type 2 diabetic patients is closely related to hepatic insulin resistance, irrespective of body type. *Cardiovasc Diabetol* 2009; **8**:44.
3 Albu JB, Murphy L, Frager DH, Johnson JA, Pi-Sunyer FX. Visceral fat and race-dependent health risks in obese nondiabetic premenopausal women. *Diabetes* 1997; **46**:456–462.
4 Basu A, Basu R, Shah P, Vella A, Rizza RA, Jensen MD. Systemic and regional free fatty acid metabolism in type 2 diabetes. *Am J Physiol Endocrinol Metab* 2001; **280**:E1000–E1006.
5 Lê KA, Mahurkar S, Alderete TL, Hasson RE, Adam TC, Kim JS, *et al*. Subcutaneous adipose tissue macrophage infiltration is associated with hepatic and visceral fat deposition, hyperinsulinemia, and stimulation of NF-κB stress pathway. *Diabetes* 2011; **60**:2802–2809.
6 Shoelson SE, Lee J, Goldfine AB. Inflammation and insulin resistance. *J Clin Invest* 2006; **116**:1793–1801.
7 Hotamisligil GS. Inflammation and metabolic disorders. *Nature* 2006; **444**:860–867.
8 Love C, Tomas MB, Tronco GG, Palestro CJ. FDG PET of infection and inflammation. *Radiographics* 2005; **25**:1357–1368.
9 Zhuang H, Duarte PS, Pourdehand M, Shnier D, Alavi A. Exclusion of chronic osteomyelitis with F-18 fluorodeoxyglucose positron emission tomographic imaging. *Clin Nucl Med* 2000; **25**:281–284.
10 Kwee TC, Kwee RM, Alavi A. FDG-PET for diagnosing prosthetic joint infection: systematic review and meta-analysis. *Eur J Nucl Med Mol Imaging* 2008; **35**:2122–2132.
11 Bleeker-Rovers CP, Vos FJ, Mudde AH, Dofferhoff AS, de Geus-Oei LF, Rijnders AJ, *et al*. A prospective multi-centre study of the value of FDG-PET as part of a structured diagnostic protocol in patients with fever of unknown origin. *Eur J Nucl Med Mol Imaging* 2007; **34**:694–703.
12 Braun JJ, Kessler R, Constantinesco A, Imperiale A. ^{18}F-FDG PET/CT in sarcoidosis management: review and report of 20 cases. *Eur J Nucl Med Mol Imaging* 2008; **35**:1537–1543.
13 Christen T, Sheikine Y, Rocha VZ, Hurwitz S, Goldfine AB, Di Carli M, Libby P. Increased glucose uptake in visceral versus subcutaneous adipose tissue revealed by PET imaging. *JACC Cardiovasc Imaging* 2010; **3**:843–851.
14 Lee SJ, Seo HJ, Cheon GJ, Kim JH, Kim EE, Kang KW, *et al*. Usefulness of integrated PET/MRI in head and neck cancer: a preliminary study. *Nucl Med Mol Imaging* 2014; **48**:98–105.
15 Yoshizumi T, Nakamura T, Yamane M, Islam AH, Menju M, Yamasaki K, *et al*. Abdominal fat: standardized technique for measurement at CT. *Radiology* 1999; **211**:283–286.
16 Armstrong IS, Tonge CM, Arumugam P. Impact of point spread function modeling and time-of-flight on myocardial blood flow and myocardial flow reserve measurements for rubidium-82 cardiac PET. *J Nucl Cardiol* 2014; **21**:467–474.
17 Snijder MB, Visser M, Dekker JM, Seidell JC, Fuerst T, Tylavsky F, *et al*. The prediction of visceral fat by dual-energy X-ray absorptiometry in the elderly: a comparison with computed tomography and anthropometry. *Int J Obes Relat Metab Disord* 2002; **26**:984–993.
18 Tanaka S, Yoshiyama M, Imanishi Y, Nakahira K, Hanaki T, Naito Y, *et al*. MR measurement of visceral fat: assessment of metabolic syndrome. *Magn Reson Med Sci* 2006; **5**:207–210.
19 Kobayashi J, Tadokoro N, Watanabe M, Shinomiya M. A novel method of measuring intra-abdominal fat volume using helical computed tomography. *Int J Obes Relat Metab Disord* 2002; **26**:398–402.
20 Hamdy O, Porramatikul S, Al-Ozairi E. Metabolic obesity: the paradox between visceral and subcutaneous fat. *Curr Diabetes Rev* 2006; **2**:367–373.
21 Berker Y, Franke J, Salomon A, Palmowski M, Donker HC, Temur Y, *et al*. MRI-based attenuation correction for hybrid PET/MRI systems: a 4-class tissue segmentation technique using a combined ultrashort-echo-time/Dixon MRI sequence. *J Nucl Med* 2012; **53**:796–804.
22 Ng JM, Azuma K, Kelley C, Pencek R, Radikova Z, Laymon C, *et al*. PET imaging reveals distinctive roles for different regional adipose tissue depots in systemic glucose metabolism in nonobese humans. *Am J Physiol Endocrinol Metab* 2012; **303**:E1134–E1141.
23 Virtanen KA, Iozzo P, Hällsten K, Huupponen R, Parkkola R, Janatuinen T, *et al*. Increased fat mass compensates for insulin resistance in abdominal obesity and type 2 diabetes: a positron-emitting tomography study. *Diabetes* 2005; **54**:2720–2726.
24 Sears B, Ricordi C. Anti-inflammatory nutrition as a pharmacological approach to treat obesity. *J Obes* 2011; **2011**:431985.